EUROPEAN RESPIRATORY *journal*

FLAGSHIP SCIENTIFIC JOURNAL OF ERS

Early View

Original research article

Respiratory effort during sleep and prevalent hypertension in obstructive sleep apnoea

Jean-Benoit Martinot, Nhat-Nam Le-Dong, Atul Malhotra, Jean-Louis Pépin

Please cite this article as: Martinot J-B, Le-Dong N-N, Malhotra A, *et al*. Respiratory effort during sleep and prevalent hypertension in obstructive sleep apnoea. *Eur Respir J* 2022; in press (https://doi.org/10.1183/13993003.01486-2022).

Respiratory effort during sleep and prevalent hypertension in obstructive sleep apnoea

Jean-Benoit Martinot[1,2], Nhat-Nam Le-Dong[3], Atul Malhotra[4], Jean-Louis Pépin[5]

[1]Sleep Laboratory, CHU Université Catholique de Louvain (UCL) Namur Site Sainte-Elisabeth, Namur, Belgium

[2]Institute of Experimental and Clinical Research, UCL Bruxelles Woluwe, Brussels, Belgium

[3]Sunrise, Namur, Belgium

[4]University of California San Diego, La Jolla, CA, USA

[5]HP2 Laboratory, Inserm U1300, University Grenoble Alpes, Grenoble, France

Corresponding author: Jean-Benoit Martinot, Centre du Sommeil et de la Vigilance, CHU-UCL Namur Site Ste Elisabeth, 15 Place Louise Godin, 5000 Namur, Belgium. Tel +32 495502608. Fax +32 81570754. Email martinot.j@respisom.be

"Take Home" message

The proportion of sleep time spent with increased respiratory effort automatically derived from mandibular movements was a better predictor of prevalent hypertension in patients with OSA than traditional PSG metrics (e.g. AHI).

ABSTRACT

Mechanisms underlying blood pressure changes in obstructive sleep apnoea (OSA) are incompletely understood. Increased respiratory effort (RE) is one of the main features of OSA and is associated with sympathetic overactivity, leading to increased vascular wall stiffness and remodelling. This study investigated associations between a new measure of RE (percentage of sleep time spent with increased RE based on measurement of mandibular jaw movements [MJM]; REMOV, %TST) and prevalent hypertension in adults referred for evaluation of suspected OSA.

A machine learning model was built to predict hypertension from clinical data, conventional polysomnography (PSG) indices, and MJM-derived parameters (including REMOV, %TST). The model was evaluated in a training subset and a test subset.

The analysis included 1127 patients, 901 (80%) in the training subset and 226 (20%) in the test subset. The prevalence of hypertension was 31% and 30%, respectively, in the training and test subsets. A risk stratification model based on eighteen input features including REMOV had good accuracy for predicting prevalent hypertension (sensitivity 0.75, specificity 0.83). Using the Shapley additive explanation (SHAP) method, REMOV was the best predictor of hypertension after clinical risk factors (age, sex, body mass index, neck circumference) and time with oxygen saturation <90%, ahead of standard PSG metrics (including the apnoea-hypopnoea index and oxygen desaturation index).

The proportion of sleep time spent with increased RE automatically derived from MJM was identified as a potential new reliable metric to predict prevalent hypertension in patients with OSA.

Key words: obstructive sleep apnoea; hypertension; respiratory effort; mandibular jaw movements

Introduction

Obstructive sleep apnoea (OSA) is a highly prevalent condition [1] that is associated with a variety of adverse consequences, including excessive daytime sleepiness [2], cognitive dysfunction [3] and cardiovascular disease [4], especially hypertension [5-7].

The main acute physiological consequences of OSA are intermittent hypoxia, intrathoracic pressure changes generated by increased respiratory effort (RE), and arousals [8]. Increased RE is therefore a key component of obstructive apnoeas and hypopnoeas, and respiratory event-related arousals (RERAs). The apnoea-hypopnoea index (AHI) has traditionally been used to estimate OSA severity, and describes the average number of respiratory events occurring per hour of sleep. However, the AHI does not convey relevant information about hypoxic burden and total sleep time (TST) spent with increased RE despite the fact that these metrics have been linked to OSA cardiovascular and mortality outcomes [9,10]. As a result, it is now widely accepted that the AHI is unable to capture fully the complex pathophysiological processes of OSA [11,12], and that more comprehensive and combined metrics are required to define fully cardiovascular risk in a given patient with OSA.

The role of increased RE in cardiovascular mortality has been poorly studied to date. The only physiological data currently available show that intrathoracic pressure swings during respiratory events generate subsequent sympathetic nervous system overactivity [13,14], and might accelerate arterial stiffness and arterial wall remodelling. In addition, currently available evidence suggests that RE contributes to increases in nocturnal blood pressure [15-25].

The lack of data on the cardiovascular impact of increased RE can be partly explained by the challenge of assessing and measuring the proportion of total sleep time (TST) spent in RE. We have previously demonstrated that mandibular jaw movements (MJM) during sleep

provide powerful information about RE and sleep time spent in increased RE [26,27]. In normal physiological sleep, the mandibular jaw slightly moves a few tenths of a millimetre at the breathing frequency around a fixed position and the mouth is almost closed. This sleep physiological displacement is controlled by the respiratory and pre-motor trigeminal nuclei and reflects respiratory drive and variations in respiratory efforts. MJM therefore reflect respiratory drive level and efforts as a function of variations in upper airway resistance that typically occur during abnormal respiratory events [26,27].

This study evaluated the association between sleep time spent in increased RE automatically derived from measurements of MJM (REMOV %TST) and prevalent hypertension in patients being investigated for suspected OSA. We hypothesised that an increase MJM during sleep would be independently associated with hypertension beyond the classical metrics of hypoxic burden and sleep fragmentation.

Methods

Study design and population

This was a cross-sectional analysis of consenting consecutive adult patients referred for assessment of suspected OSA. The study was approved by the Comité d'Ethique Hospitalo-Facultaire-Universitaire de Liège (IRB-00004890-NB707201523388) and all participants provided written informed consent prior to enrolment.

Overnight sleep study

In-laboratory polysomnography (PSG) was recorded with a digital acquisition system (Somnoscreen Plus, Somnomedics, Rander-sacken, Germany). The parameters monitored included electroencephalogram (EEG), right and left electro-oculogram, submental

electromyogram (EMG), tibial EMG, chest and abdominal wall motion by respiratory inductance plethysmography (SleepSense S.L.P. Inc., St. Charles, IL, USA), nasal and oral flows by a pressure transducer and a thermistor, respectively, and oxygen saturation (SpO_2) by a digital oximeter displaying pulse wave form (Nonin, Nonin Medical, Plymouth, MN, USA).

PSG recordings were manually scored by two experienced investigators who were unaware of participant identity. All sleep stages, EEG arousals and sleep-related respiratory events were visually scored in based on American Academy of Sleep Medicine criteria [28,29]. OSA diagnosis was confirmed based on ICSD-3 criteria and required either signs/symptoms or related medical/psychiatric disorder together with ≥5 predominantly obstructive respiratory events (i.e., obstructive and mixed apnoeas, hypopnoeas or RERAs; referred to as PSG_ORDI) per hour of sleep. Alternatively, occurrence of ≥15 obstructive respiratory events of per hour was sufficient to diagnose OSA, even in the absence of associated symptoms or disorders [30]. The conventional rules for severity grading based on AHI were used to categorize into non-OSA (<5), mild (5-15), moderate (15-30) and severe OSA (>30) [12]. Inter-observer agreement for PSG scoring was evaluated by intra-class correlation coefficient using two-way random model for single measure (ICC 2.1); this was 92.1% (95% confidence interval [CI] 0.891–0.942; p<0.001).

Mandibular jaw movement recordings

MJM were recorded using the Sunrise system (Sunrise, Namur, Belgium). This is composed of a coin-sized tri-axial gyroscopic sensor that was attached to the patient's chin between the inferior labial sulcus and the pogonion by the sleep technician. An embedded inertial measurement unit enables MJM sensing and communicates with a smartphone application

for external control. Displacement of the mandible is calculated from the integration of the rotational speed measured by a gyroscope. The position of the mandible resulting from elevation or depression is determined by an accelerometer. These three inertial measurement units provide six derived channels in total.

MJM signal automated machine learning algorithms were trained with a large number of fragments obtained from periods of normal breathing and epochs that included the full spectrum of obstructive events (RERAs, obstructive apnoeas, obstructive hypopnoeas and mixed episodes) and central events. Details of absolute values generated by the Sunrise system have been reported previously [27].

MJM data were automatically transferred to a cloud-based infrastructure at the end of the night, and data analysis was performed using a dedicated machine-learning algorithm. This algorithm is designed to identify automatically obstructive and mixed apnoea/hypopnoea or RERA based on stereotypical MJM patterns. It automatically processes MJM signal components and determines whether MJM patterns could be classified as sleep, arousal or wake. To identify wake, the algorithm tested whether MJM signals were fast, irregular and non-predictable [31]. For the identification of arousal movements, the algorithm detected brisk MJM of large amplitude indicating the abrupt closure of the mouth characteristic of arousals [31,32].

Respiratory effort burden

This new metric provides an indication of the time spent in RE assessed using MJM. Periods of increased RE were identified through oscillating MJM of increased and variable amplitudes at the breathing frequency [26,27] (Figure 1). The MJM algorithm identifies respiratory disturbances as a period of RE ended by an arousal or an awakening. The

Sr_ORDI consists of the total number of respiratory disturbances accompanied by RE as a proportion of TST, is estimated from the Sunrise analytics [33]. The new variable is RE during sleep based on MJM measurement as a proportion of TST (REMOV %TST).

Prevalent hypertension outcome

A sleep specialist performed a clinical examination in the morning (between 8:30am and 12:00pm) during which blood pressure was measured three times with the patient seated in a quiet room. All medications were recorded in an electronic medical record. History, office blood pressure and medication usage were used to define hypertension status. The presence of hypertension was defined as a documented history of hypertension and treatment with at least one antihypertensive drug.

Data analysis

Data preparation, exploratory analysis, model development, validation and interpretation were carried out using Python programming language. The data analytics plan is summarised in Figure 2. Key elements are as follows.

1) Data splitting and optimisation of machine learning algorithm

The dataset was randomly divided into two subsets: a larger set for model development and a smaller set for secondary independent validation. We built a binary classification rule to recognize patients with co-morbid hypertension based on input data for eighteen anthropometric features and sleep studies indices: male sex (binary value), age, body mass index (BMI), neck circumference, Epworth Sleepiness Scale (ESS) score, nine PSG-derived indices (TST, respiratory disturbance index [RDI], obstructive RDI [ORDI], AHI, obstructive AHI [OAHI], oxygen desaturation index [ODI], arousal index [ArI], proportion of TST spent

with SpO_2 <90% or <95%), and four indices provided by Sunrise's automatic MJM signal analysis (Sr_TST, Sr_ArI, Sr_ORDI and REMOV).

The extreme gradient boosting (XGB) classifier algorithm was adopted for this classification task (see Supplemental Methods in the online supplement for more details). The learning objective is set as a binary classification, with hypertension as the positive label. The training implied a gradient tree booster and histogram optimised approximate greedy tree construction algorithm.

(2) Cross-validation on training set

The model's performance was evaluated using the 10-fold cross-validation procedure, which implied multiple data splitting and random resampling, thus allowing unbiased evaluation of model performance on 10% of unseen data.

(3) Secondary validation on independent dataset

A final model was trained on the whole training set using the optimised parameter values. This model was validated on unseen data in the testing subset. The following evaluations were conducted for both repeated k-folds cross-validation and independent validation: normalised confusion matrix (to evaluate model accuracy – the rows represent the true observation, and the columns indicate the classification by model); and conventional metrics for evaluating the binary classification accuracy and diagnostic efficiency, including sensitivity, specificity, F1-score (harmonic mean between sensitivity and positive predictive value [PPV]), balanced accuracy (BAC), positive/negative likelihood ratios (LR+, LR-), PPV, negative predictive value (NPV) and area under the receiver operating characteristic curve (ROC AUC).

(4) Model explanation and evaluation of features contribution

To evaluate the contribution of each feature to the model final prediction, the Lundberg Shapley additive explanation (SHAP) method was applied [34]. This method unifies the concept of Shapley values from the cooperative game theory (1953) with a local interpretation approach. The SHAP method allows depiction of the respective power of association of different factors on the explanatory variable (in this case hypertension). It also allows inclusion of all variables of interest even if collinearity exists between some of the variables.

The association between RE burden and the risk of comorbid hypertension was also explored using a conventional statistical inference based on regression coefficients from a 10-fold cross-validation of Ridge logistic regression model. The model implies a linear regression with binomial distribution and a L2 regularisation, which provides more stable parameters.

Results

Study population

A total of 1127 subjects were included in the study, 901 (80%) in the training subset and 226 (20%) in the test subset (Table 1). The prevalence of hypertension was 31% and 30%, respectively, in the training and test subsets. In the training subset, mean blood pressure was 136/82 mmHg in patients with hypertension and 128/78 mmHg in those without hypertension (Table 1); six patients met the criteria for resistant hypertension. Patients with versus without hypertension differed in several clinical characteristics and respiratory parameters (Table 1).

Clinical characteristics and RE burden

Clear differences in the distribution of a variety of features based on the presence or absence of hypertension (Figure 3A) provides an indication of the potential for association between that feature and hypertension. The features were categorised by their pathophysiological characteristic and method of measurement (PSG or Sunrise system) and were combined with anthropometric parameters influencing blood pressure (as described in the Methods section).

The PSG-derived ORDI and ArI metrics distribution and the corresponding MJM-derived indices reflecting number of events and desaturation were similarly distributed between the groups with and without HTN (Figure 3A). RE burden (REMOV %TST) was higher in patients with versus without hypertension (Figure 3A), suggesting a high ability of REMOV to differentiate between patients with and without hypertension. On principal component analysis, TST and the ESS score did not contribute to hypertension risk, whereas other respiratory measures and demographic/clinical features were associated with the presence of hypertension (Figure 3B).

Machine learning model for predicting prevalent hypertension

A machine learning model including a variety of anthropometric parameters and physiological features from PSG and Sunrise technology, showed good performance for the prediction of hypertension in the test subset (Table 2). The final model showed good performance in the test subset, with a ROC AUC of 0.88 (95% CI 0.85–0.9), sensitivity of 0.75 (0.66–0.83) and specificity of 0.83 (0.78–0.88) (Figure 4, Table 2). A ROC without REMOV showed worse performance with respect to the sensitivity/specificity trade-off (Figure S1, Table S1).

Model explanation by SHAP method

The five strongest predictors of prevalent hypertension in patients with OSA were age, male sex, time with SpO_2 <90%, BMI and neck circumference (Figure 5). The three next most important contributors were REMOV, Sr_ORDI and PSG_ORDI (Figure 5). These were followed by other PSG indices (in descending order of importance): PSG_TST, time with SpO_2 <95%, PSG_OAHI and PSG_ArI (Figure 5).

Of these metrics, only REMOV and Sr_ORDI showed a clear asymmetric pattern in SHAP values distribution, where the highest values of REMOV and Sr_ORDI would drive positive prediction of hypertension. In contrast, SHAP values were cumulated at the centre for most PSG indices, indicating a mixed, inconsistent and less effective contribution of these metrics to the model prediction. On average, the contribution of REMOV to hypertension prediction was approximatively twice that of PSG_ORDI, PSG_AHI or ODI.

The ranking of predictive features was consistent in Ridge logistic regression analysis, which confirmed the important association between RE and the risk of hypertension (Figure S2). RE for >60% of the night remained an independent predictor of hypertension even in the absence of oxygen desaturation and when sleep fragmentation was limited (Figure S3).

Discussion

The novel finding of this study was that RE detected by MJM analysis was independently and strongly associated with prevalent hypertension in a large clinical cohort of patients with OSA. RE burden was a stronger predictor of hypertension than common PSG-derived metrics such as the AHI. While RE was not the only, or the strongest, predictor of hypertension in patients with OSA, the current data provide a more comprehensive picture of the

intermediary mechanisms and factors contributing to the development of hypertension in this patient group.

There is a pathophysiological rationale for the observed association between increased RE during sleep and hypertension. Obstructive events during sleep are the consequence of partial or complete collapse of the upper airway. These alterations in upper airway patency result in repetitive forced inspiration against the obstructed upper airway with substantial negative changes in intrathoracic pressures [20,23]. These large intrathoracic pressure swings not only generate sympathetic activation but also generate significant shear stress and vessel wall remodelling. The impact of increased respiratory effort has been poorly studied and is probably underestimated as a risk factor for OSA-related hypertension. The current findings showed that RE load was an independent predictor of prevalent hypertension in OSA beyond intermittent hypoxia. Therefore, we suggest the utility of a pragmatic tool using MJM for objectively measuring sleep time spent with increased RE. This seems like the most appropriate tool given that increased respiratory effort is poorly documented by respiratory bands with clear overestimation of central events in obese patients [35]. Snoring is a qualitative and indirect surrogate of increased respiratory effort, and inspiratory flow limitation reflects an increase in upper airway resistance. However, there is not a linear relationship between increase in RE and flattening of the inspiratory curve [36].

Based on indirect assessment of RE-related snoring or flow limitation, it has been suggested that increased nocturnal RE may play a role in the occurrence of hypertension in several different clinical scenarios, including upper airway resistance syndrome (UARS), OSA in children, and preeclampsia [37-39]. In UARS, measures of nasal flow limitation have been associated with hypertension independently of the AHI [37,40]. Also, several studies have

postulated that snoring and RERAs are associated with significant daytime sleepiness and have repercussions in cardiovascular risk [37,41,42]. In these situations, hypoxic burden is limited and treatment indications for CPAP or oral appliances are still the subject of debate. Reliable and convenient assessment of RE burden throughout the night might allow better risk stratification and personalised treatment solutions in these contexts.

Beyond suppression of intermittent hypoxia and apnoeas and hypopnoeas, the goal of CPAP titration is the full normalisation of RE, allowing complete restoration of sleep architecture [37,43]. This effect contributes to the suppression of persistent sleepiness during CPAP therapy [43] and our study suggests that this might be necessary to improve blood pressure control in patients with OSA. Prospective evaluation of the effects of CPAP therapy blood pressure in patients with evidence of increased RE but without significant oxygen desaturations or sleep fragmentation would also be an interesting area for future research.

Large intrathoracic pressure swings related to RE particularly affect intrathoracic blood vessels, including the aorta. RE not only favours the development of hypertension, as shown in our study, but might in the long run trigger or exacerbate the progression of aortic dilatation [44]. In addition, a recent meta-analysis suggested an association between OSA and aortic enlargement [45]. RE is probably a major contributor to this association, and the risk is particularly relevant in at-risk populations such as those with previous aortic dissection [46-48]. Better control of diurnal and nocturnal hypertension [49] and the reduction of intrathoracic pressure swings might help to slow the progression of aortic dilation in patients with concomitant OSA.

Our study was conducted in a large consecutive prospective sample covering the broad spectrum of OSA. This suggests that our results have good external validity, but additional validation in other cohorts is desirable. Previous studies in the field have been conducted

using less reliable measurement of RE, namely snoring and flow limitation. In contrast, our quantitative and direct estimation of RE level with MJM analytics has been validated against PSG [33] and provides a new metric indicating the total RE load during sleep. Although an association between RE and hypertension was documented, we do not have 24-hour ambulatory blood pressure data so cannot determine whether increased nocturnal RE is specifically associated with nocturnal hypertension.

In conclusion, our study highlights the underestimated role of RE as a risk factor for prevalent hypertension in OSA. RE load is an independent risk factor for hypertension beyond classical anthropometric cardiovascular risk factors and usual PSG metrics. Risk stratification using new metrics beyond AHI is the new paradigm in OSA [49], and our data suggest that RE based on measurement of MJM, allowing objective measurement of sleep time spent with RE, should be included in the range of new indices for OSA management. This measurement is of particular interest in specific populations such as those with UARS without desaturations or in patients with cardiovascular diseases at high risk for aortic expansion and dissection. A digital medicine solution incorporating MJM and artificial intelligence analysis is ready to operate with home recordings over multiple nights of evaluation, before and after therapeutic interventions.

Acknowledgments

The authors wish to thank Ms. Ravzat Ashurlaeva and Ms. Bao Truc Nguyen Ham for their secretarial assistance and support. English language editing and formatting assistance was provided by Nicola Ryan, independent medical writer.

Funding support and role of the sponsor

J-L.P. is supported by the French National Research Agency in the framework of the "Investissements d'avenir" program (ANR-15-IDEX-02) and the "e-health and integrated care and trajectories medicine and MIAI artificial intelligence" chairs of excellence from the Grenoble Alpes University Foundation. This work has been partially supported by MIAI @ Grenoble Alpes, (ANR-19-P3IA-0003).

The first draft of the manuscript was prepared by JLP and JBM, who had unrestricted access to the data. The manuscript was reviewed and edited by all the authors. All authors made the decision to submit the manuscript for publication and assume responsibility for the accuracy and completeness of the analyses and for the fidelity of this report to the trial protocol. JLP has personally reviewed the data, understands the statistical methods employed for all analyses, and confirms an understanding of these analyses, that the methods are clearly described and that they are a fair way to report the results.

Competing interests

JBM reports being a scientific advisor to Sunrise and being an investigator in pharmacy trials for Jazz Pharmaceuticals, Theranexus and Desitin. NNLD is an employee of Sunrise. AM is funded by NIH, reports income related to medical education from Livanova, Equillium, Jazz, Sunrise; ResMed provided a philanthropic donation to UCSD. JLP reports being a scientific advisor to Sunrise; receiving grants and/or personal fees from ResMed, Philips, Fisher & Paykel, Sefam, AstraZeneca, AGIR à dom, Elevie, VitalAire, Boehringer Ingelheim, Jazz Pharmaceuticals, and Itamar Medical Ltd; and receiving research support for clinical studies from Mutualia and Air Liquide Foundation.

Author contributions

All authors helped revise the manuscript and approved it for submission. All authors made a significant contribution to the work reported, whether that is in the conception, study design, execution, acquisition of data, analysis and interpretation, or in all these areas; took part in drafting, revising or critically reviewing the article; gave final approval of the version to be published; have agreed on the journal to which the article has been submitted; and agree to be accountable for all aspects of the work.

Figure Legends

FIGURE 1: 15-minute fragment of recording showing mandibular jaw movements during increased respiratory effort across sleep disordered breathing.

From left to right, a typical period of respiratory effort-related arousal (RERA) is seen during the first 4 minutes where inspiratory flow limitation is clearly seen on the nasal pressure channel with snoring while the abdomino-thoracic belts remain synchronous. The respiratory displacements of the mandible are well captured by the gyroscope (gyr) and the accelerometer (acc), showing a mild increase in respiratory effort. During periods of stable flow limitation, the amplitude of the mandibular displacement increases as a function of the intensity of effort. In contrast, after short awakening, there are successive central apnoeas (blue arrows). During central apnoeas, mandibular movements decrease dramatically and can disappear until arousal occurs. Then, there are obstructive apnoeas (red arrows) and hypopnoeas (green arrows) that are accompanied by a greater increase in respiratory effort (see amplitude of mandibular movements) in parallel with desynchronization of the belts. Highlighted portions, A and B, are shown in more detail in the online supplement (Figure S4 A&B). SpO_2, oxygen saturation.

FIGURE 2: Overview of the experimental and analysis protocol.

SHAP, Shapley additive explanation method; XGB, extreme gradient boosting.

FIGURE 3: Distribution of clinical features and principal component analysis (PCA).

(A) Density plots showing the distribution of twelve features that showed the most significant difference between participants with or without hypertension; (B) Loading plot summarising the PCA. The graph consists of a bi-dimensional density layer, representing the

joint distribution of two principal components (PC), and coordinates of the seventeen original variables as vectors, including age, body mass index (BMI), neck circumference, Epworth Sleepiness Scale (ESS) score, nine PSG-derived indices (TST, respiratory disturbance index [RDI], obstructive RDI [ORDI], AHI, obstructive AHI [OAHI], oxygen desaturation index [ODI], arousal index [ArI], proportion of TST spent with SpO_2 <90% or <95%), and four indices provided by Sunrise's automatic MJM signal analysis (Sr_TST, Sr_ArI, Sr_ORDI and REMOV). Each vector represents a variable; its orientation with respect to a principal component axis and length indicate how much the variable contributes to that PC. The angles between the vectors and direction allow evaluation of their correlation: small angles indicate strong positive correlation; opposite angles represent a negative correlation.

FIGURE 4: Global performance of model, based on RKF cross-validation and independent data.

a) Average normalised confusion matrix obtained from 100 replications of extreme gradient boosting model in a 10-fold cross-validation; b) Normalised confusion matrix based on application of the final model on unseen data from 226 subjects; c) Receiver operating characteristic (ROC) curve evaluating the global performance of the final model on an independent testing subset.

AUC, area under the curve; Negative, hypertension absent; Positive, hypertension present.

FIGURE 5: Contribution of the eighteen input features to the classification output, evaluated by the Shapley additive explanation (SHAP) method.

The bar graph on the left compares the average impact of a feature on model output magnitude. Each bar indicates the average of absolute SHAP values for a specific feature in

all individual cases. For the graph on the right, the x-axis represents the SHAP value scale, which is proportional to the probability of having hypertension. Each dot indicates the feature attribution value to the extreme gradient boosting model final prediction score for a respective patient. The dots are coloured according to the relative value of a specific feature, in which blue (cooler) or red (warmer) dots represent lower or higher feature values, respectively.

AHI, apnoea-hypopnoea index; ArI, arousal index; BMI, body mass index; circ., circumference; Desat_dt <90% or <95%, time with oxygen saturation <90% or <95%; ESS, Epworth Sleepiness Scale; OAHI, obstructive apnoea-hypopnoea index; ODI, oxygen desaturation index; ORDI, obstructive respiratory disturbance index; PSG, derived from polysomnography; RDI, respiratory disturbance index; REMOV, proportion of total sleep time with increased respiratory effort during sleep (based on mandibular movement measurement); Sr, derived from automatic analysis of mandibular movements by the Sunrise system; TST, total sleep time.

Tables

TABLE 1: Characteristics of study population

Parameters	Training subset (n=901; 80%)		Test subset (n=226; 20%)	
	Hypertension (n=279; 31%)	**Without hypertension (n=622; 69%)**	**Hypertension (n=68; 30%)**	**Without hypertension (n=158; 70%)**
Male sex, n (%)	129 (46.2)	265 (42.3)	35 (46.2)	80 (42.6)
Age, years	56.58±15.72	44.17±18.24	55.06±13.03	44.57±17.70
Neck circumference, cm	41.00±5.00	39.00±5.00	40.00±3.00	39.00±5.00
Systolic BP, mmHg	135.7±17.1	128.0±12.4	138.4±22.3	125.4±14.5
Diastolic BP, mmHg	82.1±13.6	78.2±11.9	80.9±17.2	75.9±11.1
BMI, kg/m^2	32.87±10.17	28.52±11.06	31.78±9.52	30.15±10.30
ESS score	11.00±8.00*	11.00±7.00	10.00±7.00*	11.00±6.00
OSA severity, n (%)				
Non-severe	19 (6.8)	104 (16.7)	4 (5.9)	27 (15.2)
Mild	49 (17.6)	223 (35.8)	13 (19.1)	57 (32.0)
Moderate	81 (29.0)	149 (24.0)	22 (32.4)	39 (21.9)
Severe	130 (46.6)	146 (23.5)	29 (42.6)	55 (30.9)
PSG indices				
TST, min	420.52±109.76*	437.27±98.12	415.76±76.13	430.75±89.87
ArI, n/h	29.57±23.71	22.89±17.45	28.96±22.40	22.96±16.98
AHI, n/h	27.32±29.12	14.00±22.31	26.52±27.90	14.04±19.64
OAHI, n/h	19.44±27.99	9.87±19.23	19.18±26.45	9.26±16.71
RDI, n/h	34.33±31.29	20.84±24.70	32.76±27.54	21.28±21.18
ORDI, n/h	26.73±27.00	15.84±21.42	27.95±25.84	16.26±18.58
ODI, n/h	24.86±35.26	10.73±23.01	23.87±32.97	9.54±20.94
Time with SpO_2 <90%, % TST	3.43±12.90	0.28±3.06	4.35±9.73	0.36±3.79
Time with SpO_2 <95%, % TST	19.45±22.4	7.63±16.03	17.88±21.80	7.38±15.35
Sunrise indices				
TST, min	439.00±81.25*	439.74±75.73	450.75±65.25	439.25±68.00
ORDI, n/h	20.66±15.20	13.50±14.34	22.52±16.80	13.62±13.01
ArI, n/h	21.97±16.16	17.79±13.55	23.35±21.42	17.24±13.69
REMOV, % TST	75.96±26.96	56.05±47.95	77.34±26.40	55.41±43.83
Antihypertensive medication, n (%)				
Beta blockers	127 (45.5)	-	54 (79.4)	-

ACEI	79 (28.3)	-	38 (55.9)	-
ARB	71 (25.4)	-	27 (39.7)	-
CCB	87 (31.2)	-	14 (20.6)	-
Diuretic	63 (25.6)	-	19 (27.9)	-
Other	12 (4.3)	-	1 (1.5)	-
Number of antihypertensives, n (%)				
None	-	622 (100.0)	-	158 (100.0)
1	176 (63.1)	-	13 (19.1)	-
2	52 (18.6)	-	31 (45.6)	-
3	46 (16.5)	-	18 (26.5)	-
4	4 (1.4)	-	6 (8.8)	-
5	1 (0.4)	-	-	-

Values are mean ± standard deviation or number of patients (%).

* All metrics, except for TST (PSG & Sunrise) and ESS showed a statistically significative difference in distribution between two outcome subgroups, based on a Mann-Whitney test at significance threshold of 0.005.

ACEI, angiotensin-converting enzyme inhibitor; AHI, apnoea-hypopnoea index; ARB, angiotensin receptor blocker; ArI, arousal index; BMI, body mass index; CCB, calcium channel blocker; Desat_dt, time with oxygen saturation <90% or <95%; ESS, Epworth Sleepiness Scale; OAHI, obstructive apnoea-hypopnoea index; ODI, oxygen desaturation index; ORDI, obstructive respiratory disturbance index; OSA, obstructive sleep apnoea; PSG, polysomnography; RDI, respiratory disturbance index; REMOV, respiratory effort during sleep (based on mandibular movement measurement); SpO_2, oxygen saturation; TST, total sleep time.

TABLE 2: Evaluation of model performance by repeated 10-fold cross-validation and independent validation on test subset

Metrics	Repeated 10-fold cross-validation (n=901)		Independent validation on test set (n=226)	
	Estimated	**95% CI**	**Estimated**	**95% CI**
F1 score	0.76	0.70–0.81	0.70	0.62–0.77
Balanced accuracy	0.76	0.71–0.81	0.79	0.74–0.84
Sensitivity	0.77	0.69–0.85	0.75	0.66–0.83
Specificity	0.75	0.67–0.83	0.83	0.78–0.88
PPV	0.25	0.17–0.33	0.17	0.12–0.22
NPV	0.23	0.15–0.31	0.25	0.17–0.34
LR+	3.17	2.33–4.32	4.52	3.29–6.21
LR-	0.30	0.19–0.40	0.30	0.19–0.41
ROC AUC	0.84	0.79–0.89	0.88	0.85–0.90

CI, confidence interval; LR, likelihood ratio; NPV, negative predictive value; PPV, positive predictive value; ROC AUC, area under the receiver operator characteristics curve.

References

1. Benjafield AV, Ayas NT, Eastwood PR, et al. Estimation of the global prevalence and burden of obstructive sleep apnoea: a literature-based analysis. Lancet Respir Med 2019: 7: 687-698.
2. Jennum P, Coaquira Castro J, Mettam S, et al. Socioeconomic and humanistic burden of illness of excessive daytime sleepiness severity associated with obstructive sleep apnoea in the European Union 5. Sleep Med 2021: 84: 46-55.
3. Alomri RM, Kennedy GA, Wali SO, et al. Association between nocturnal activity of the sympathetic nervous system and cognitive dysfunction in obstructive sleep apnoea. Sci Rep 2021: 11: 11990.
4. Linz D, Woehrle H, Bitter T, et al. The importance of sleep-disordered breathing in cardiovascular disease. Clin Res Cardiol 2015: 104: 705-718.
5. Lavie P, Herer P, Hoffstein V. Obstructive sleep apnoea syndrome as a risk factor for hypertension: population study. BMJ 2000: 320: 479-482.
6. Nieto FJ, Young TB, Lind BK, et al. Association of sleep-disordered breathing, sleep apnea, and hypertension in a large community-based study. Sleep Heart Health Study. JAMA 2000: 283: 1829-1836.
7. Peppard PE, Young T, Palta M, et al. Prospective study of the association between sleep-disordered breathing and hypertension. N Engl J Med 2000: 342: 1378-1384.
8. Kohler M, Stradling JR. Mechanisms of vascular damage in obstructive sleep apnea. Nat Rev Cardiol 2010: 7: 677-685.
9. Azarbarzin A, Sands SA, Stone KL, et al. The hypoxic burden of sleep apnoea predicts cardiovascular disease-related mortality: the Osteoporotic Fractures in Men Study and the Sleep Heart Health Study. Eur Heart J 2019: 40: 1149-1157.

10. Butler MP, Emch JT, Rueschman M, et al. Apnea-Hypopnea Event Duration Predicts Mortality in Men and Women in the Sleep Heart Health Study. Am J Respir Crit Care Med 2019: 199: 903-912.
11. Lévy P, Tamisier R, Pépin JL. Assessment of sleep-disordered-breathing: Quest for a metric or search for meaning? J Sleep Res 2020: 29: e13143.
12. Malhotra A, Ayappa I, Ayas N, et al. Metrics of sleep apnea severity: beyond the apnea-hypopnea index. Sleep 2021: 44.
13. Ryan S. Mechanisms of cardiovascular disease in obstructive sleep apnoea. J Thorac Dis 2018: 10: S4201-s4211.
14. Weiss JW, Remsburg S, Garpestad E, et al. Hemodynamic consequences of obstructive sleep apnea. Sleep 1996: 19: 388-397.
15. Ali NJ, Davies RJ, Fleetham JA, et al. The acute effects of continuous positive airway pressure and oxygen administration on blood pressure during obstructive sleep apnea. Chest 1992: 101: 1526-1532.
16. Berry RB, Asyali MA, McNellis MI, et al. Within-night variation in respiratory effort preceding apnea termination and EEG delta power in sleep apnea. J Appl Physiol (1985) 1998: 85: 1434-1441.
17. Fletcher EC. The relationship between systemic hypertension and obstructive sleep apnea: facts and theory. Am J Med 1995: 98: 118-128.
18. Hoffstein V, Chan CK, Slutsky AS. Sleep apnea and systemic hypertension: a causal association review. Am J Med 1991: 91: 190-196.
19. Issa FG, Sullivan CE. Upper airway closing pressures in snorers. J Appl Physiol Respir Environ Exerc Physiol 1984: 57: 528-535.

20. Magder SA, Lichtenstein S, Adelman AG. Effect of negative pleural pressure on left ventricular hemodynamics. Am J Cardiol 1983: 52: 588-593.

21. Peters J, Kindred MK, Robotham JL. Transient analysis of cardiopulmonary interactions. I. Diastolic events. J Appl Physiol (1985) 1988: 64: 1506-1517.

22. Peters J, Kindred MK, Robotham JL. Transient analysis of cardiopulmonary interactions. II. Systolic events. J Appl Physiol (1985) 1988: 64: 1518-1526.

23. Sforza E, Krieger J, Petiau C. Nocturnal evolution of respiratory effort in obstructive sleep apnoea syndrome: influence on arousal threshold. Eur Respir J 1998: 12: 1257-1263.

24. Stradling JR, Barbour C, Glennon J, et al. Which aspects of breathing during sleep influence the overnight fall of blood pressure in a community population? Thorax 2000: 55: 393-398.

25. Young T, Finn L, Hla KM, et al. Snoring as part of a dose-response relationship between sleep-disordered breathing and blood pressure. Sleep 1996: 19: S202-205.

26. Martinot JB, Le-Dong NN, Cuthbert V, et al. Mandibular Movements As Accurate Reporters of Respiratory Effort during Sleep: Validation against Diaphragmatic Electromyography. Front Neurol 2017: 8: 353.

27. Pepin JL, Le-Dong NN, Cuthbert V, et al. Mandibular Movements are a Reliable Noninvasive Alternative to Esophageal Pressure for Measuring Respiratory Effort in Patients with Sleep Apnea Syndrome. Nat Sci Sleep 2022: 14: 635-644.

28. Berry RB, Brooks R, Gamaldo C, et al. AASM Scoring Manual Updates for 2017 (Version 2.4). J Clin Sleep Med 2017: 13: 665-666.

29. Berry RB, Budhiraja R, Gottlieb DJ, et al. Rules for scoring respiratory events in sleep: update of the 2007 AASM Manual for the Scoring of Sleep and Associated Events.

Deliberations of the Sleep Apnea Definitions Task Force of the American Academy of Sleep Medicine. J Clin Sleep Med 2012: 8: 597-619.

30. American Academy of Sleep Medicine. Inernational Classification of Sleep Disorders. 3rd ed. American Academy of Sleep Medicine, Darien, IL, 2014.
31. Martinot JB, Borel JC, Cuthbert V, et al. Mandibular position and movements: Suitability for diagnosis of sleep apnoea. Respirology 2017: 22: 567-574.
32. Le-Dong NN, Martinot JB, Coumans N, et al. Machine Learning-based Sleep Staging in Patients with Sleep Apnea Using a Single Mandibular Movement Signal. Am J Respir Crit Care Med 2021: 204: 1227-1231.
33. Pépin JL, Letesson C, Le-Dong NN, et al. Assessment of Mandibular Movement Monitoring With Machine Learning Analysis for the Diagnosis of Obstructive Sleep Apnea. JAMA Netw Open 2020: 3: e1919657.
34. Lundberg SM, Erion G, Chen H, et al. From Local Explanations to Global Understanding with Explainable AI for Trees. Nat Mach Intell 2020: 2: 56-67.
35. Boudewyns A, Willemen M, Wagemans M, et al. Assessment of respiratory effort by means of strain gauges and esophageal pressure swings: a comparative study. Sleep 1997: 20: 168-170.
36. Pamidi S, Redline S, Rapoport D, et al. An Official American Thoracic Society Workshop Report: Noninvasive Identification of Inspiratory Flow Limitation in Sleep Studies. Ann Am Thorac Soc 2017: 14: 1076-1085.
37. Pépin JL, Guillot M, Tamisier R, et al. The upper airway resistance syndrome. Respiration 2012: 83: 559-566.

38. Guilleminault C, Winkle R, Korobkin R, et al. Children and nocturnal snoring: evaluation of the effects of sleep related respiratory resistive load and daytime functioning. Eur J Pediatr 1982: 139: 165-171.

39. Edwards N, Blyton DM, Kirjavainen T, et al. Nasal continuous positive airway pressure reduces sleep-induced blood pressure increments in preeclampsia. Am J Respir Crit Care Med 2000: 162: 252-257.

40. Guilleminault C, Stoohs R, Shiomi T, et al. Upper airway resistance syndrome, nocturnal blood pressure monitoring, and borderline hypertension. Chest 1996: 109: 901-908.

41. Asker M, Asker S, Kucuk U, et al. An overlooked cause of resistant hypertension: upper airway resistance syndrome - preliminary results. Clinics (Sao Paulo) 2014: 69: 731-734.

42. Guilleminault C, Kirisoglu C, Poyares D, et al. Upper airway resistance syndrome: a long-term outcome study. J Psychiatr Res 2006: 40: 273-279.

43. Meurice JC, Paquereau J, Denjean A, et al. Influence of correction of flow limitation on continuous positive airway pressure efficiency in sleep apnoea/hypopnoea syndrome. Eur Respir J 1998: 11: 1121-1127.

44. Gaisl T, Bratton DJ, Kohler M. The impact of obstructive sleep apnoea on the aorta. Eur Respir J 2015: 46: 532-544.

45. Gherbesi E, Tadic M, Faggiano A, et al. Sleep Apnea Syndrome and Large Artery Subclinical Damage: Targeting Thoracic Aortic Dilatation. Am J Hypertens 2022: 35: 543-550.

46. Barone-Rochette G, Thony F, Boggetto-Graham L, et al. Aortic Expansion Assessed by Imaging Follow-up after Acute Aortic Syndrome: Effect of Sleep Apnea. Am J Respir Crit Care Med 2015: 192: 111-114.

47. Delsart P, Soquet J, Pierache A, et al. Influence of nocturnal hypoxemia on follow-up course after type B acute aortic syndrome. BMC Pulm Med 2021: 21: 401.

48. Delsart P, Soquet J, Drumez E, et al. Aortic root size is associated with nocturnal blood pressure in a population of hypertensive patients under treatment for obstructive sleep apnea. Sleep Breath 2019: 23: 439-446.

49. Pépin JL, Eastwood P, Eckert DJ. Novel avenues to approach non-CPAP therapy and implement comprehensive obstructive sleep apnoea care. Eur Respir J 2022: 59.

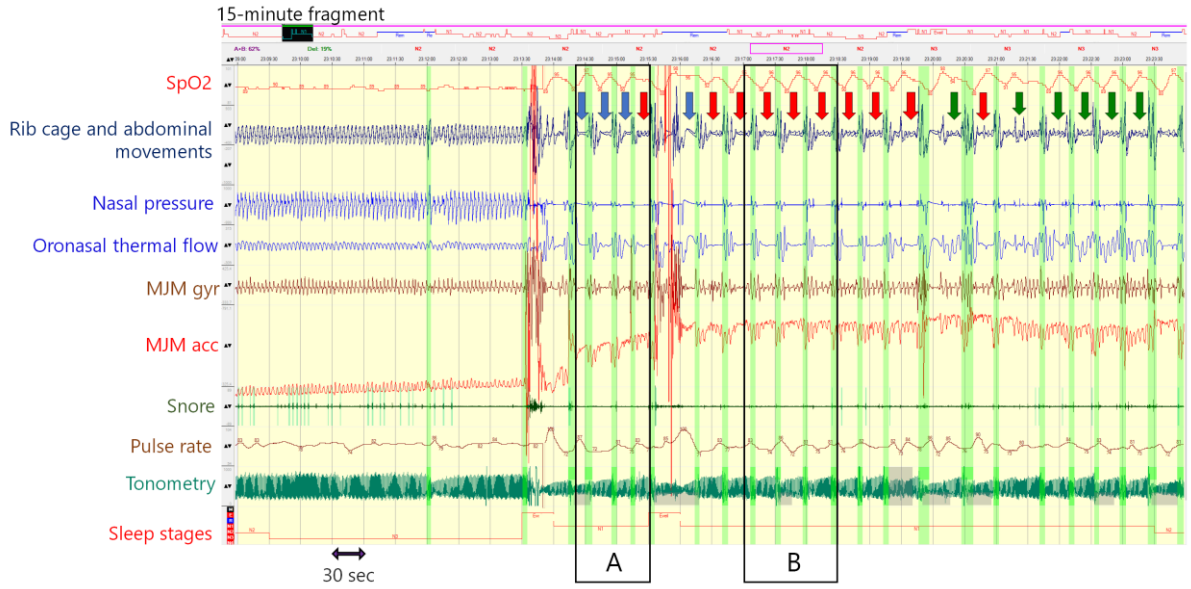
15-minute fragment
SpO2
Rib cage and abdominal movements
Nasal pressure
Oronasal thermal flow
MJM gyr
MJM acc
Snore
Pulse rate
Tonometry
Sleep stages
30 sec
A
B

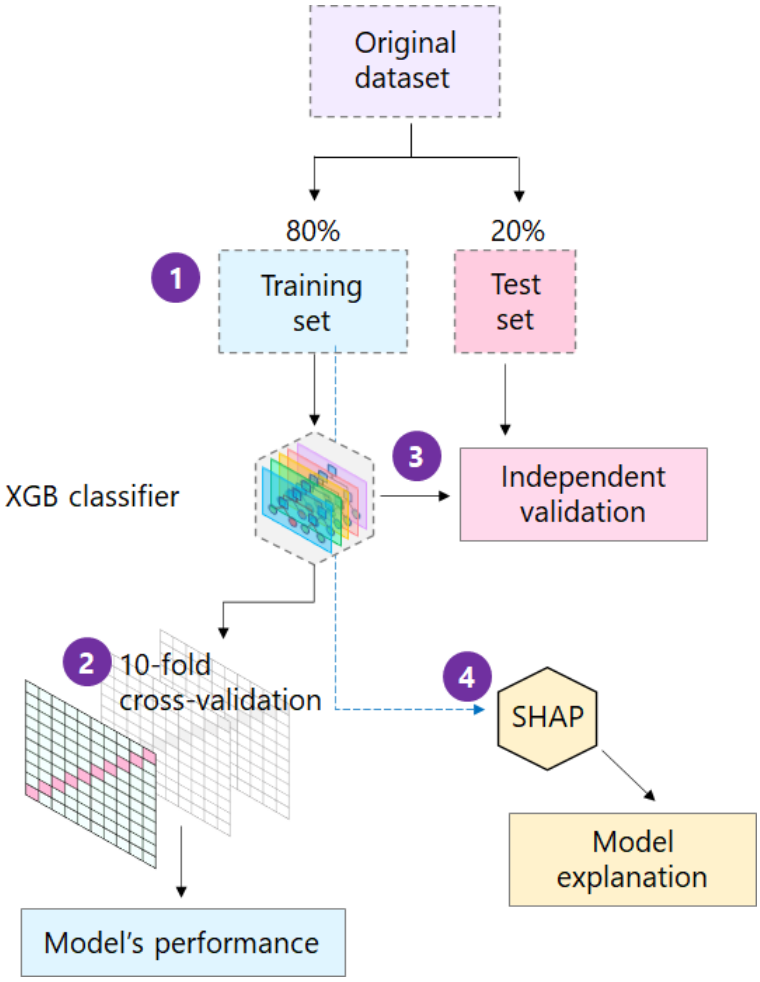
Original dataset
80%
20%
1
Training set
Test set
XGB classifier
3
Independent validation
2
10-fold cross-validation
4
SHAP
Model explanation
Model's performance

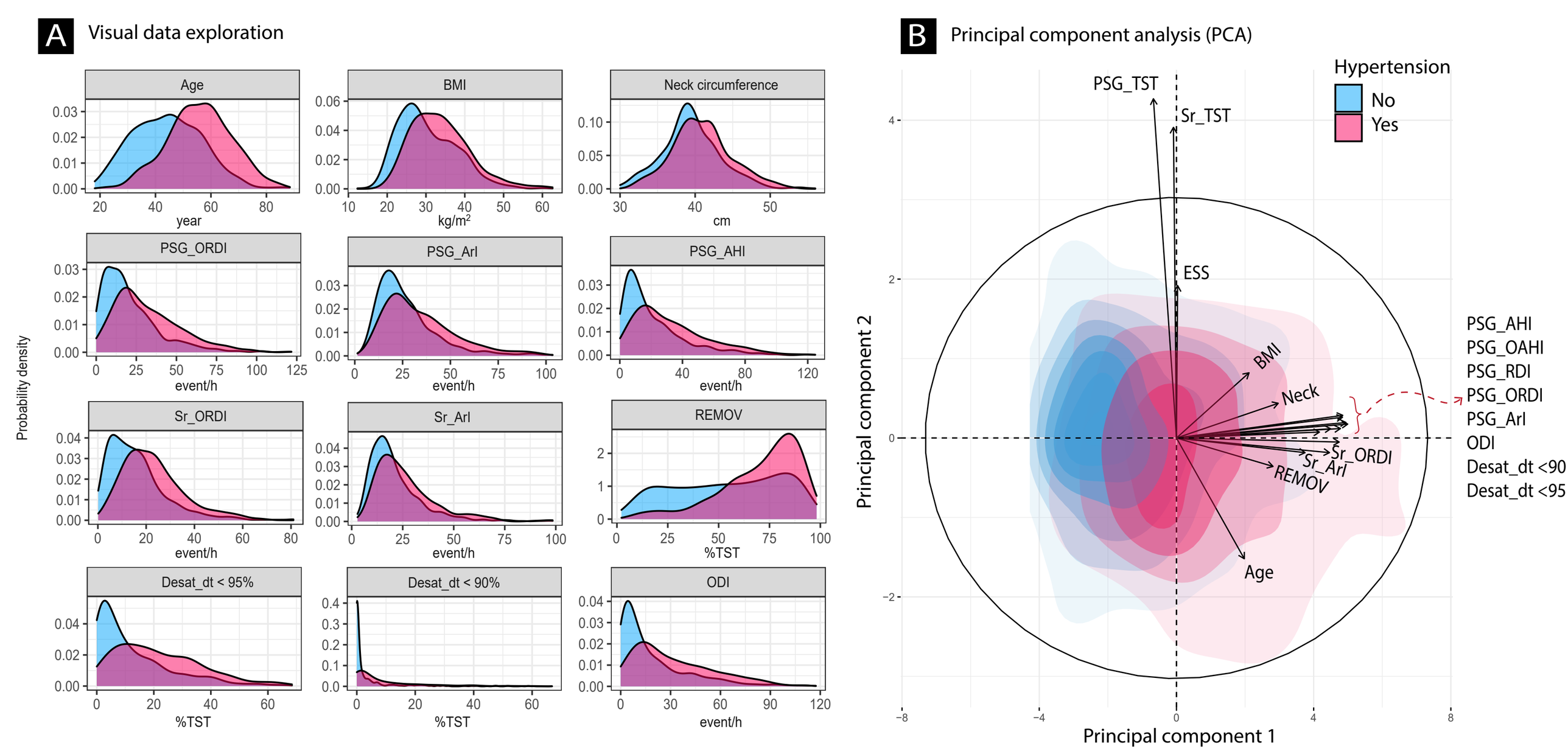
A
Visual data exploration
Age
BMI
Neck circumference
PSG_ORDI
PSG_ArI
PSG_AHI
Sr_ORDI
Sr_ArI
REMOV
Desat_dt < 95%
Desat_dt < 90%
ODI
Probability density
year
kg/m²
cm
event/h
%TST
B
Principal component analysis (PCA)
Hypertension
No
Yes
PSG_TST
Sr_TST
ESS
BMI
Neck
Sr_ORDI
Sr_ArI
REMOV
Age
PSG_AHI
PSG_OAHI
PSG_RDI
PSG_ORDI
PSG_ArI
ODI
Desat_dt <90
Desat_dt <95
Principal component 1
Principal component 2

a) Cross-validation

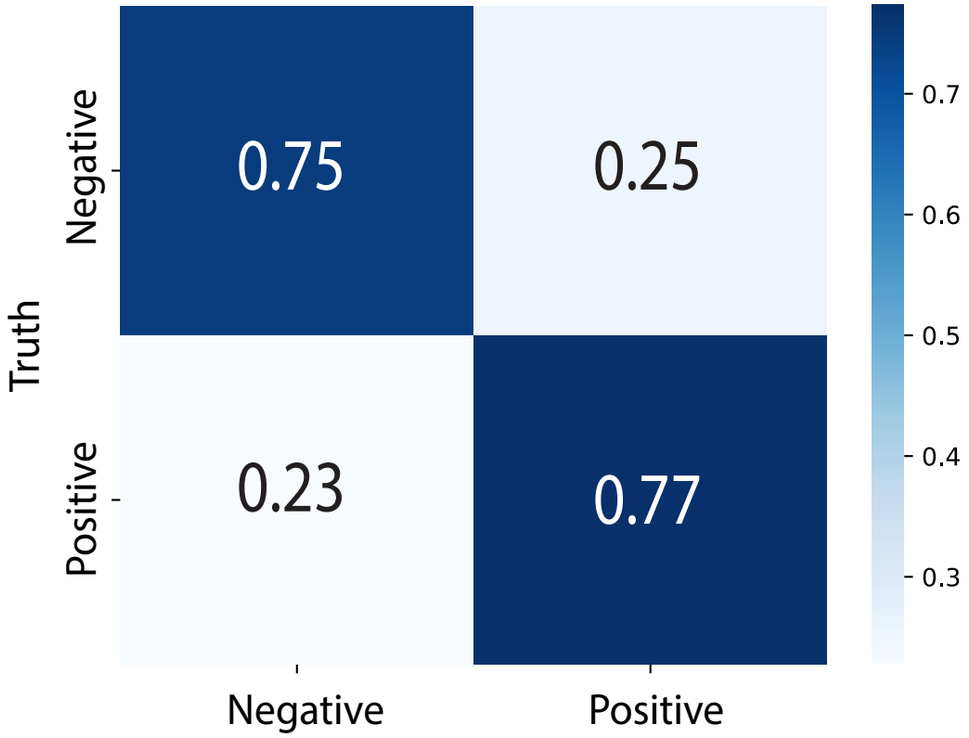

b) Independent test subset

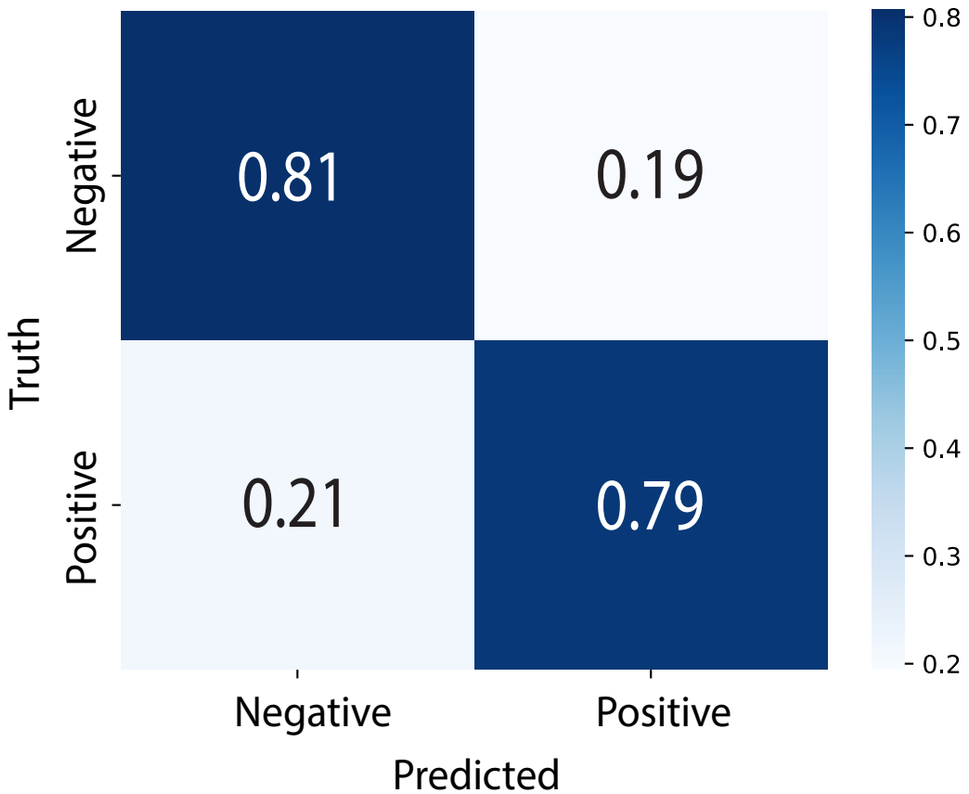

c) ROC curve on independent test subset

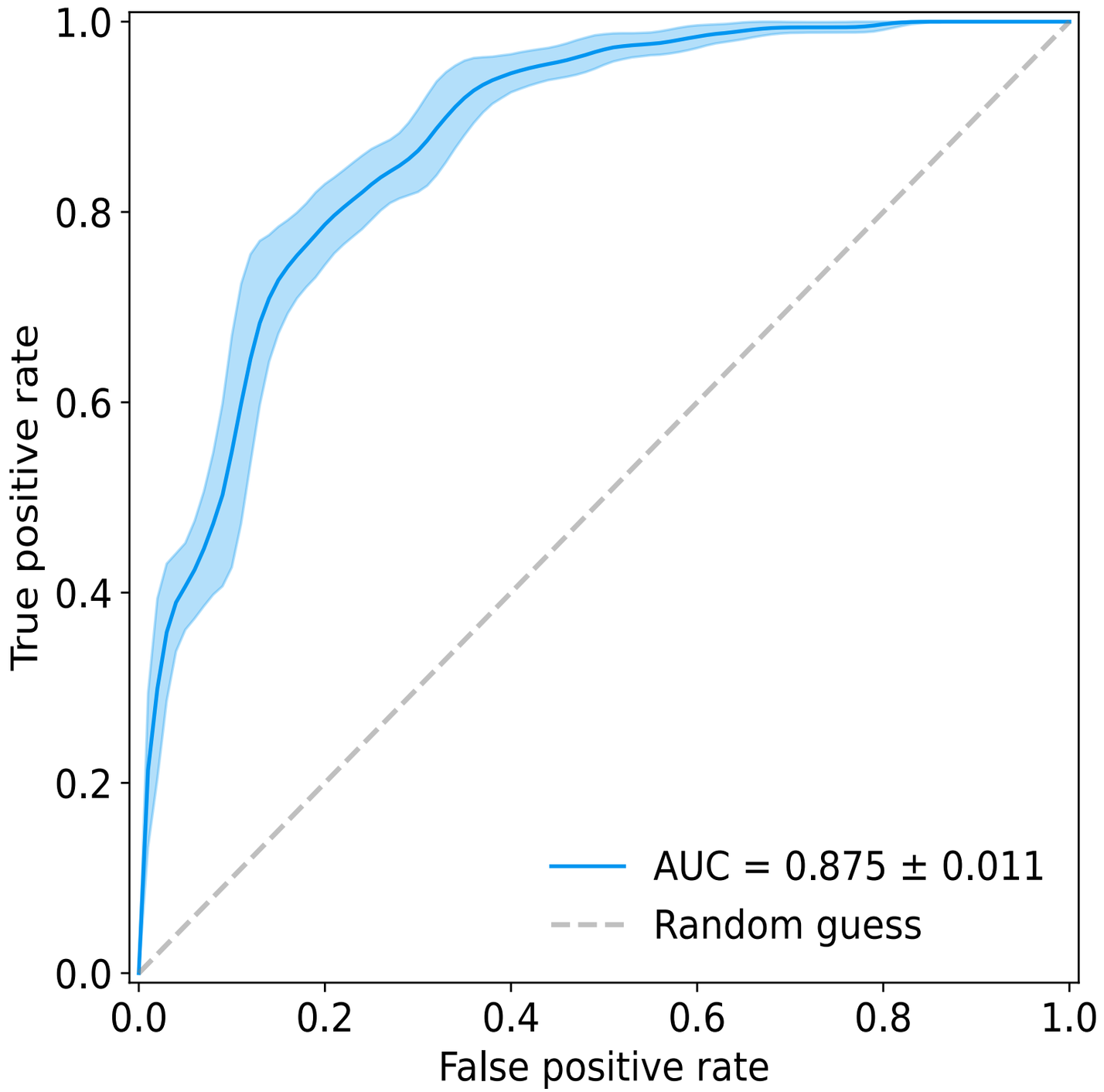

Note: Positive = with hypertension
Negative = without hypertension

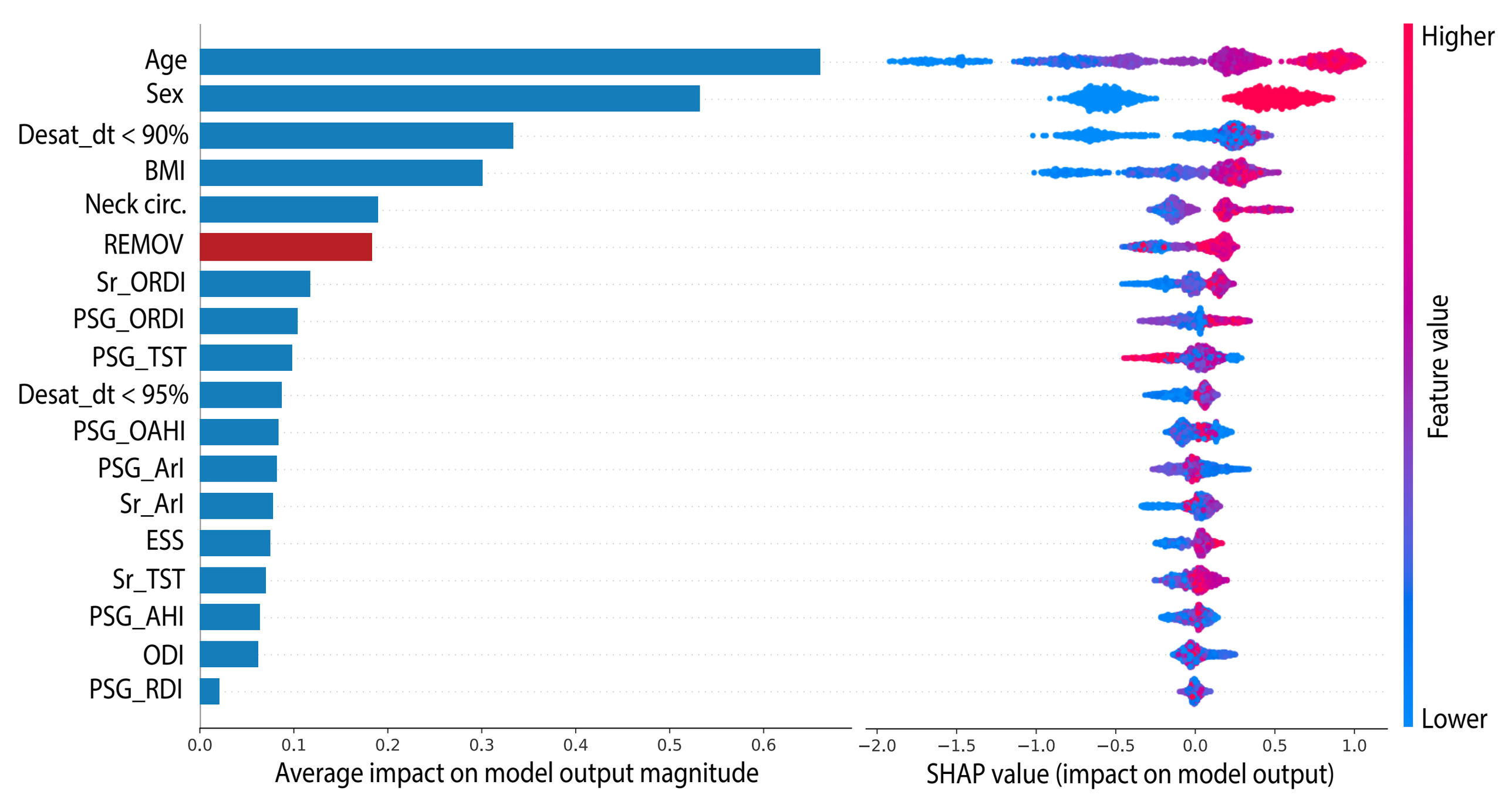
Age
Sex
Desat_dt < 90%
BMI
Neck circ.
REMOV
Sr_ORDI
PSG_ORDI
PSG_TST
Desat_dt < 95%
PSG_OAHI
PSG_ArI
Sr_ArI
ESS
Sr_TST
PSG_AHI
ODI
PSG_RDI
0.0
0.1
0.2
0.3
0.4
0.5
0.6
Average impact on model output magnitude
−2.0
−1.5
−1.0
−0.5
0.0
0.5
1.0
SHAP value (impact on model output)
Higher
Feature value
Lower

ONLINE SUPPLEMENT

Respiratory effort during sleep and prevalent hypertension in obstructive sleep apnoea

Jean-Benoit Martinot[1,2], Nhat-Nam Le-Dong[3], Atul Malhotra[4], Jean-Louis Pépin[5]

[1]Sleep Laboratory, CHU Université Catholique de Louvain (UCL) Namur Site Sainte-Elisabeth, Namur, Belgium

[2]Institute of Experimental and Clinical Research, UCL Bruxelles Woluwe, Brussels, Belgium

[3]Sunrise, Namur, Belgium

[4]University of California San Diego, La Jolla, CA, USA

[5]HP2 Laboratory, Inserm U1300, University Grenoble Alpes, Grenoble, France

Supplemental methods

Gradient tree boosting is an approach where new tree-based classification rules are created to correct the errors made by existing rules until no further improvements can be made [1]. Then all rules are combined to make the final prediction and minimise the prediction error. Logarithmic loss was chosen as the evaluation metric (thus optimising the balanced accuracy between negative and positive labels). A hyperparameter tuning was performed with repeated cross-validation on training set. The best parameter configuration for training was as follow: learning rate of 0.01, maximum depth level of 5, subsample ratio of instances of 0.75. Lower learning rate allows prevention of overfitting; this will shrink the feature weights to make the boosting process more conservative. Due to the imbalanced proportion among the target labels, we balanced the training data using the synthetic minority oversampling technique (SMOTE) [2] before each training session.

Table S1. Evaluation of performance by repeated 10-fold cross-validation and independent validation on test subset for a model that does not include the proportion of total sleep time with respiratory effort during sleep based on mandibular movement measurement (REMOV).

Metrics	Repeated 10-fold cross-validation (n=901)			Independent validation on test set (n=226)		
	Estimated	**95% CI**	**p-value***	**Estimated**	**95% CI**	**Significance****
F1 score	0.76	0.69–0.81	0.713	0.62	0.54–0.70	Yes
Balanced accuracy	0.75	0.69–0.80	0.009	0.73	0.68–0.79	Yes
Sensitivity	0.80	0.71–0.89	0.996	0.73	0.65–0.82	Yes
Specificity	0.70	0.62–0.76	<0.001	0.73	0.68–0.79	Yes
PPV	0.30	0.24–0.38	<0.001	0.27	0.21–0.32	Yes
NPV	0.20	0.11–0.29	0.999	0.26	0.18–0.35	Yes
LR+	2.70	2.04–3.45	<0.001	2.81	2.18–3.61	Yes
LR-	0.29	0.16–0.43	0.931	0.36	0.24–0.49	Yes
ROC AUC	0.83	0.78–0.87	0.002	0.84	0.74–0.86	Yes

CI, confidence interval; LR, likelihood ratio; NPV, negative predictive value; PPV, positive predictive value; ROC AUC, area under the receiver operator characteristics curve.

*p-value versus full model; paired samples t-test (Table 2).

**Statistically significant versus full model; permutation test (Table 2).

Figure S1. Performance of model that does not include the proportion of total sleep time with respiratory effort during sleep based on mandibular movement measurement (REMOV), based on RKF cross-validation and independent data.

a) Average normalised confusion matrix obtained from 100 replications of extreme gradient boosting model in a 10-fold cross-validation; b) Normalised confusion matrix based on application of the final model on unseen data from 226 subjects; c) Receiver operating characteristic (ROC) curve evaluating the global performance of the final model on an independent testing subset. AUC, area under the curve; Negative, hypertension absent; Positive, hypertension present.

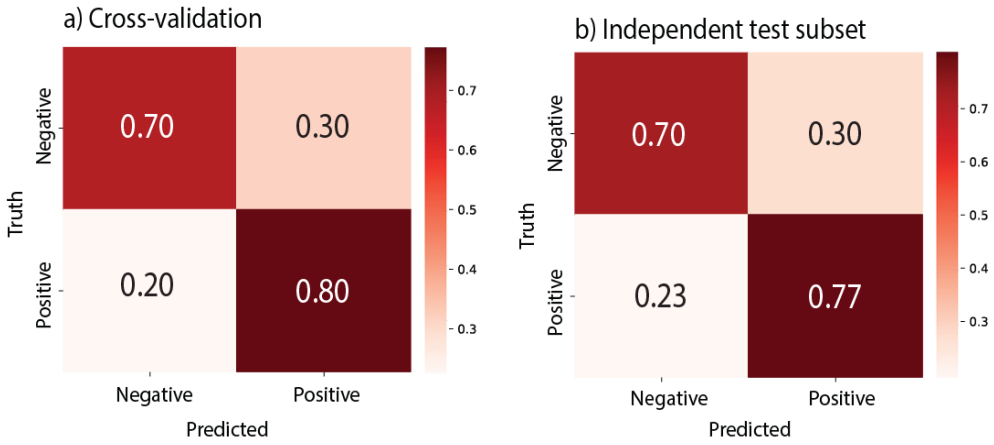

c)

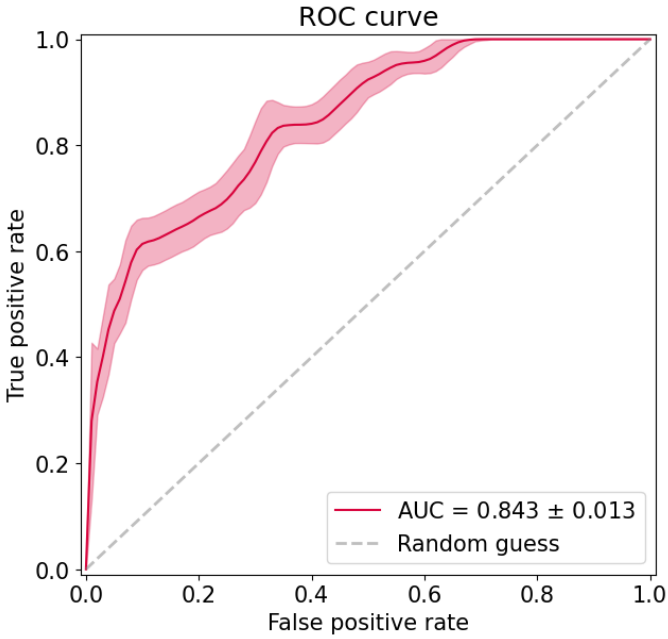

Figure S2. Ridge logistic regression analysis.

Bars show the average value of coefficients from a 10-fold cross-validation of the Ridge logistic regression model (this was a linear regression with binomial distribution and a L2 regularisation, providing more stable parameters). Higher model coefficient values indicate greater strength of association between the corresponding predictor and the risk of comorbid hypertension.

AHI, apnoea-hypopnoea index; ArI, arousal index; BMI, body mass index; circ., circumference; Desat_dt, time with oxygen saturation <90% or <95%; ESS, Epworth Sleepiness Scale; OAHI, obstructive apnoea-hypopnoea index; ODI, oxygen desaturation index; ORDI, obstructive respiratory disturbance index; PSG, derived from polysomnography; RDI, respiratory disturbance index; REMOV, respiratory effort during sleep (based on mandibular movement measurement); Sr, derived from automatic analysis of mandibular movements by the Sunrise system; TST, total sleep time.

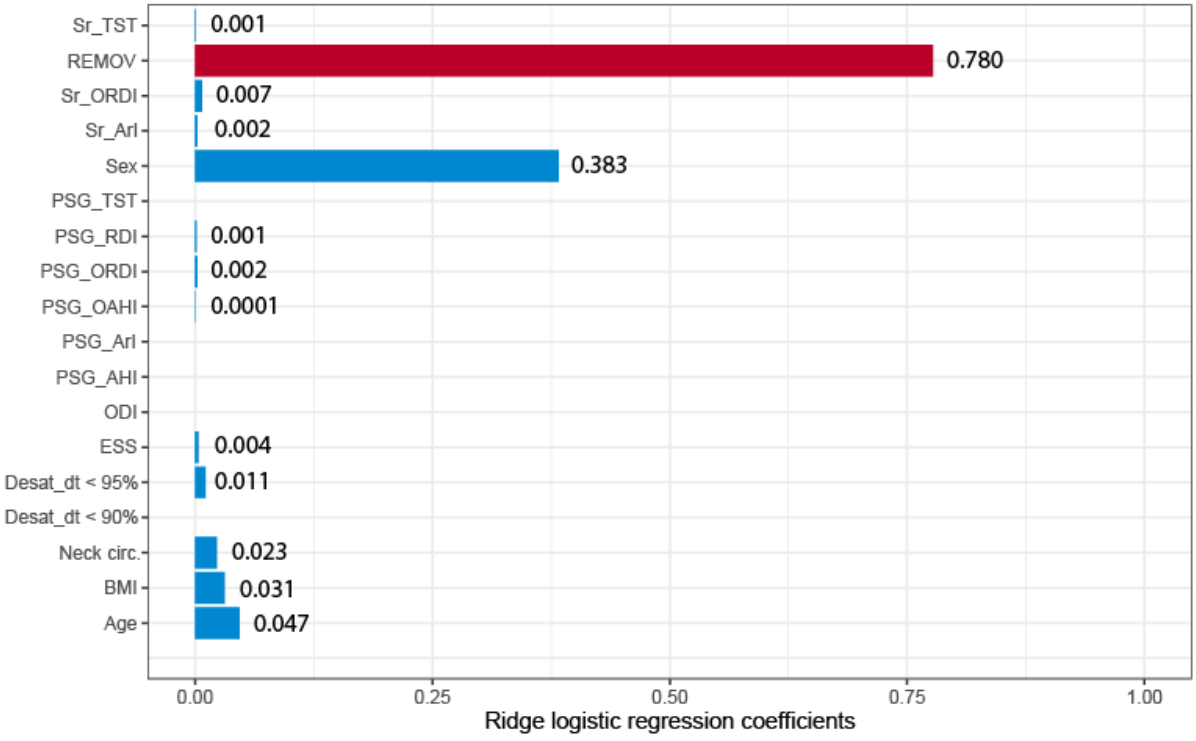

Figure S3. Shapley additive explanation method (SHAP) score for the contribution of respiratory effort duration in the absence of oxygen desaturation and when sleep fragmentation was limited. The red dots represent subjects with primary snoring and low values of the apnoea-hypopnoea index (**A**) and oxygen desaturation index (**B**) (<5 events/h). AHI, apnoea-hypopnoea index; ODI, oxygen desaturation index; REMOV, proportion of total sleep time with respiratory effort during sleep (based on mandibular movement measurement).

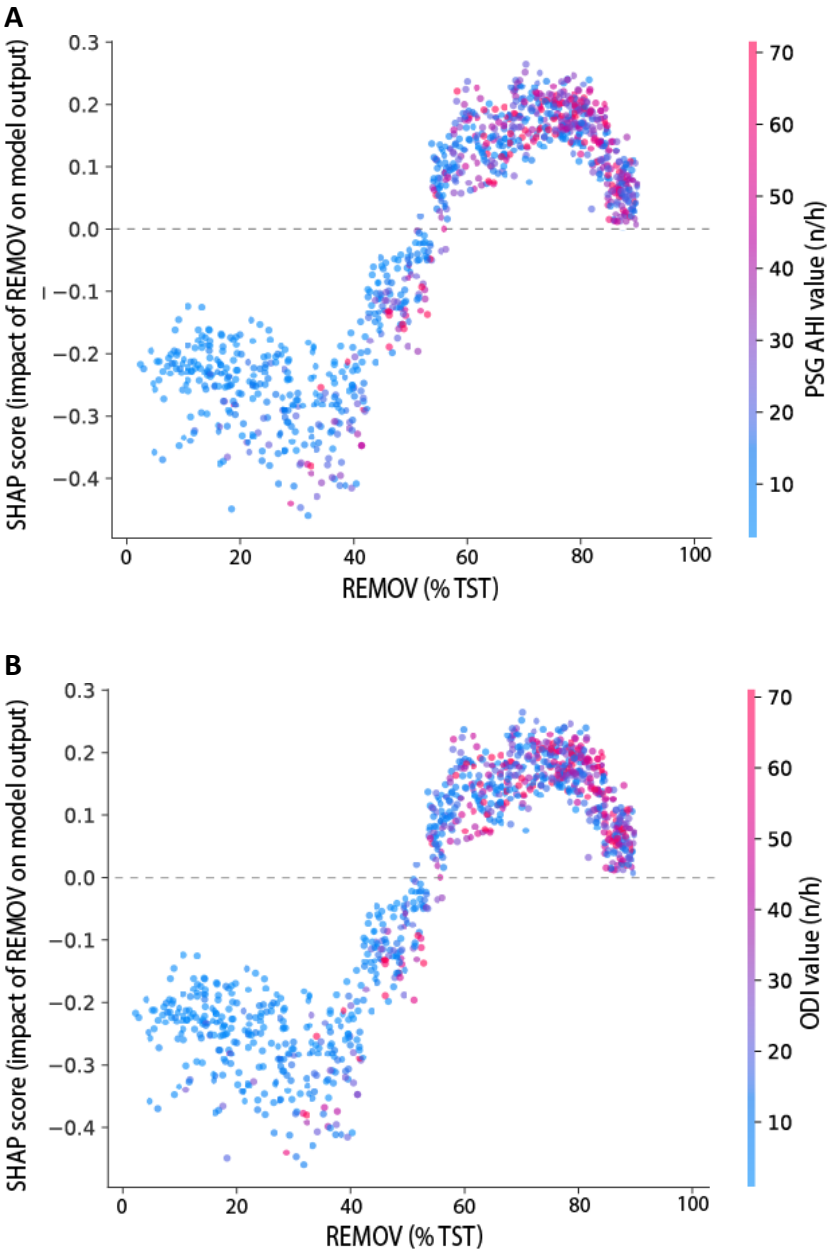

Figure S4. A) Expanded view of a 60-second recording showing mandibular jaw movements during a period of central sleep apnoeas.

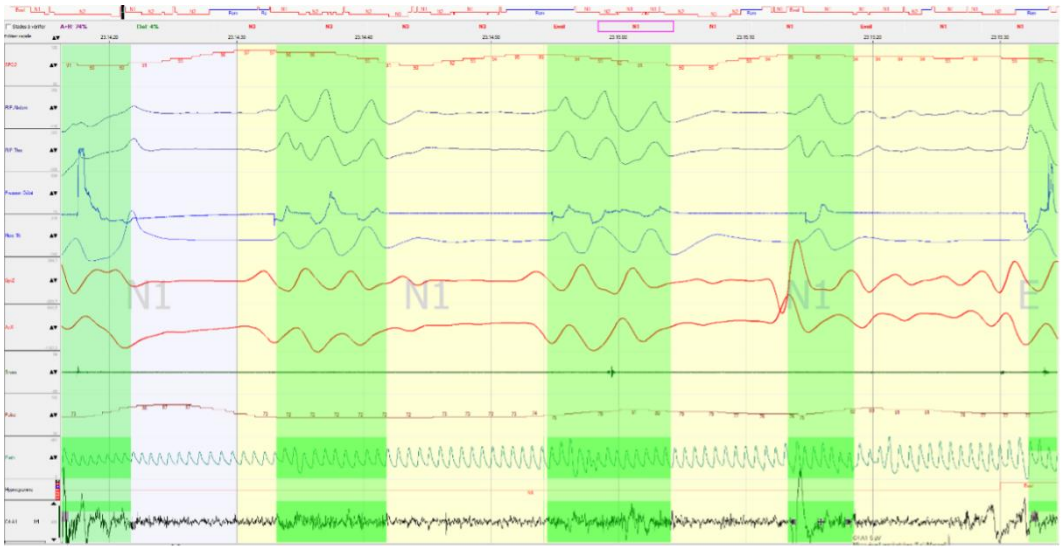

B) Expanded view of a 60-second recording showing mandibular jaw movements during a period of obstructive sleep apnoeas.

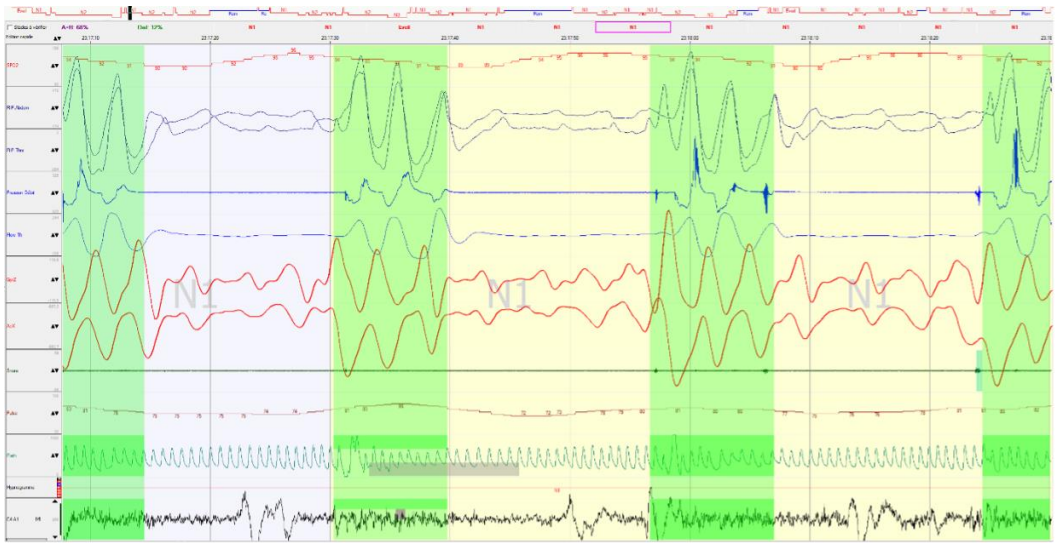

References

1. Chen T, Guestrin C. XGBoost: A Scalable Tree Boosting System. KDD '16: Proceedings of the 22nd ACM SIGKDD International Conference on Knowledge Discovery and Data Mining. August 2016. Pages 785–794.

2. Chawla NV, Bowyer KW, Hall LO, Kegelmeyer WP. SMOTE: synthetic minority over-sampling technique. *J Art Intel Res.* 2002;16:321-357.